On the Challenges of Simulating Deployable Space Structures: A Case Study

V. D. BALOPOULOS[1] and J. F. ABEL[2]

School of Civil and Environmental Engineering, Hollister Hall, Cornell University
Ithaca, New York 14853-3501, USA
Phone: +(607) 255-7582, Fax: +(607) 255-9004, E-mail: jfa5@cornell.edu

ABSTRACT

To simulate the quasi-static stowage behavior of a retractable "hingeless mast," the design and experimental testing of which have been reported by T. Kitamura *et al.* (1988), geometrically exact rod elements, the Hilber-Hughes-Taylor alpha-method of time integration, and quasi-Newton iteration with line search and automatic restarts are used. A simplified and coarsely discretized model of the mast is capable of reproducing the observed characteristics of the stowage of the mast, including the necessary buckling of the longerons and the subsequent large rigid-body and strain-related deformations. Coarse temporal discretization is found to provide sufficient accuracy if combined with the use of iterative, adaptive, and safeguarded solutions algorithms. However the presence of intermittent constraints or contact necessitates the use of extremely small analysis increments to maintain stability and accuracy and may, thus, render the simulation infeasible. Furthermore, the computed response is sensitive both to the mathematical models of the structure and applied excitation and to the employed analysis algorithms and parameters. Such analysis sensitivity parallels the sensitivity in the response of the actual structure and introduces the need for ensembles of simulations that attempt to capture and characterize the set of possible responses.

INTRODUCTION

The dynamics of space structures pose a unique combination of simulation challenges. They involve small strains but large rigid-body and strain-producing deformations, local and global instabilities, and often closely spaced equilibria. They are also strongly dependent on the behavior of various joints and deployment devices, usually modeled as kinematic constraints. The writers' objective has been to assemble, improve, and test simulation methods that might be suitable and effective for such problems, Balopoulos (1997). The principal tools selected to attack simulations of flexible space structures include: (i) geometrically exact finite element formulations for rods, cables, and a variety of constraints; (ii) methods of time integration which provide asymptotic annihilation of high frequencies and accurate modeling of low frequencies with relatively large time increments; and (iii) iterative and adaptive nonlinear solvers which employ step-safeguarding techniques to avoid divergence.

The formulations and numerical tools adopted are employed in the simulation of an actual deployable space structure, one of the recoilable and self-deploying lattice masts discussed in Kitamura *et al.* (1988) and schematically illustrated in Figure 1. These masts consist of three continuous longerons framed by integrated radial (star-like) spacers and stiffened by six

---

[1] Former Graduate Research Assistant
[2] Presenting author, Professor of Structural Engineering

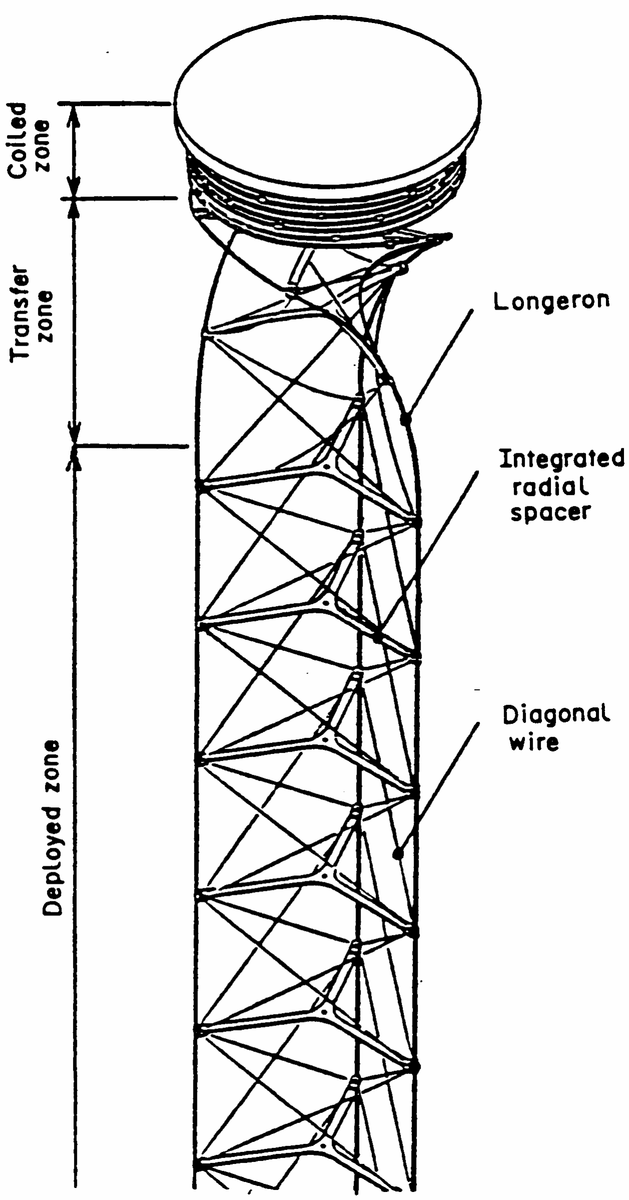

Figure 1. Schematic of a partially deployed recoilable mast [Fig. 1 of Kitamura *et al.* (1988)]

diagonal wires per bay. They are stowed by recoiling under compression, and their subsequent deployment is propelled by stored elastic strain energy. The case selected is a hingeless mast, i.e., its spacers are rigidly connected to its longerons, and stowage/deployment deformations are essentially elastic twisting of the mast. A detailed experimental study of the forces and deformation patterns associated with the stowage and deployment of hingeless masts is reported in Natori *et al.* (1986). The study establishes that the statics of actual hingeless masts are only weakly deterministic due to insensitivity of the stowage/deployment forces to the deployment ratio away from the initial buckling region and because, for constant deployment ratio and slightly varying deployment force, multiple stable equilibria with drastically different associated deformations can be achieved. Furthermore, as is typical for nonlinear systems, the deformation patterns and the transitions between them are essentially unpredictable because they are affected by imperfections in the structure or in the experimental setup. Thus, the chosen case study is sufficiently challenging for the simulation tools.

Because of the commercial importance of the recoilable masts discussed by Natori *et al.* (1986) and Kitamura *et al.* (1988), the dimensions and properties are only partially disclosed. Therefore, the experimental results can only be used for qualitative comparisons to the simulation, and for the purposes of this case study an approximate model of the hingeless mast is devised.

THE STRUCTURE AND THE SIMULATION MODEL

The hingeless mask designated as HL-3 in Kitamura *et al.* (1988) is used as the prototype for the case study. The selected approximation to this configuration has a mast radius r of 75mm, a total length L of 3,000mm, a spacer pitch h of 87 mm, and a total mass M of 0.125kg. The members have elastic sections properties listed in Table 1. The two ends of the HL-3 mast are attached to a deployment canister and an end plate, but no details about these boundary conditions are given by Kitamura *et al.* (1988). Thus a fictitious integrated spacer is assumed at each end to approximate rigid-panel conditions. Furthermore, the centers of these fictitious end-spacers are connected by a "retractable-cable" constraint that controls the evolution of the deployment ratio. When the mast is fully extended, the cable is shorter than the undeformed mast by 0.05mm and thus provides prestressing. Dynamic stowage is simulated over a time interval of 20s according to the program $d(t)/d_o = 0.1 + 0.45[1 + \cos(\pi t/20)]$. Finally the centers of all pairs of neighboring spacers are connected by "impenetrable sphere" constraints to simulate contact between longerons under local coiling conditions, Balopoulos (1997).

Table 1. Elastic Sectional Properties Of Members Of Hingeless Mast Model

Members	**EA (kN)**	**GJ_T (kN mm^2)**	**EI_{IP} (kN mm^2)**	**EI_{OP} (kN mm^2)**
Longerons	80	12	15	27
Spacers	50	3	4	40
End-Spacers	500	3	400	400
Wires	13	n/a	n/a	n/a

Table 2. Finite Element Models of the Hingeless Mast

	Full	**Simplified**
Number of nodes	148	74
No. radial spacer bars	111	37
No. longeron rod segments	108	36
No. diagonal wires	204	0
No. rigid-link constraints	37	37
Total number of elements	460	110
No. d.o.f. – quadratic elements	2,227	767
No. d.o.f. – cubic elements	3,541	1,205

Finite Element Models

The mast structure is modeled with a single geometrically exact rod element (Simo and Vu-Quoc 1988, 1991) of quadratic or cubic order for each member. The number of nodes and elements for the full model are given in Table 2. However, even with this coarse discretization made possible by the geometrically exact elements, the computational time required for the nonlinear dynamic analysis with appropriately short time step is prohibitive (see Table 3 and accompanying discussion). Instead, a simplified model, also shown in Table 2, is devised by narrowing the behavior to the experimentally observed axisymmetric stowage kinematics. The diagonal wires are ignored because they are slack during most of the stowage. Furthermore, axisymmetry is explicitly enforced by modeling only one-third of the mast and by requiring that translation and rotation of each spacer's center to be parallel to the axis of symmetry. All results reported herein are for the simplified model.

Analysis Methods

Time integration is performed by the Hilber-Hughes-Taylor α-method with $\alpha = -1/3$ for maximum high frequency dissipation, Hilber *et al.* (1977) and Hoff *et al.* (1989). In addition, Rayleigh damping is employed to provide about 0.5% critical damping in the low-frequency modes and additional dissipation in high modes. Instead of seeking buckling loads and modes by performing static increments and eigen-analysis, the kinematics are biased in the direction of a twisting buckling mode by applying two opposing 10Nmm torques statically at the two topmost spacer centers. This provides an initial imperfection in terms of a slope of roughly 3% in the top bay of the mast, and this static preload is ramped down linearly to zero between t of 0.5s and 1.5s, after the first limit point of the force in the central cable occurs. For each discretization of the mast an essentially linear static analysis must be performed to produce an initial equilibrium configuration, subject to the small pretensioning of the cable and the torques at the mast top.

At each time step, the nonlinear system solver used is the limited-memory (vector) quasi-Newton method with line searches, update evaluations, and restarts (Golub and VanLoan 1989). With an appropriate choice of time step, these techniques allow each time increment to require roughly one tangent evaluation and factorization, three to four update steps, and four or five residual evaluations. The factorization technique used is a band-preserving, symmetric Crout method ($\mathbf{L}\ \mathbf{D}\ \mathbf{L}^T$).

One drawback of the software used (Balopoulos 1997) is that it does not permit adaptive time stepping. Consequently, for too-large time increments, either equilibrium cannot be reached within tolerance, and analysis must be terminated, or an artificial impact must be accepted (reducing accuracy) in hopes that such instances will be infrequent. The simplified treatment of intermittent longeron contact in the model employed therefore limits the simulation to the range where contact is not widespread, that is, to the early stages of stowage.

The effect of the modeling and analysis factors on the analysis times is reflected in Table 3. For practical computational times, the importance of using the simplified model is evident.

Table 3. Estimated Computational Times on an HP-730 Workstation

Model:	**Full model**		**Simplified model**	
Element Order:	**quadratic**	**cubic**	**quadratic**	**cubic**
One $\mathbf{L}\ \mathbf{D}\ \mathbf{L}^T$ decomposition	180 sec	290 sec	4 sec	6 sec
20-sec stowage, 10^4 steps ($\Delta t = 0.002$sec)	14 days		1 day	
20-sec stowage, 10^5 steps ($\Delta t = 0.0002$sec)				14 days

SIMULATION RESULTS

The simulation of stowage consists of two stages. The first is the prediction of the limit load of the retracting cable connecting the end-spacers (an event that could be loosely called the axisymmetric buckling of the mast in the first 1/4 sec of the stowage), a study used to choose an appropriate time increment. The second is the simulation of post-buckling deformation.

Selection of Time Steps

In this stage, results from a variety of time steps are employed for the first 1.5 seconds of the stowage with both quadratic and cubic elements. The time step selection is based on the convergence study of both the time of occurrence and the magnitude of the limit load of the cable. In addition, by a comparison of the cumulative computational costs – in terms both of the number of configuration updates and ensuing residual evaluations needed and of the number of tangent evaluations and factorizations – the effect of the time step selection on the efficiency of the nonlinear simulation is also considered. It is determined that, for quadratic elements a Δt of no larger than 0.005 sec is required, while for cubic elements steps as large as 0.02 sec can be used but $\Delta t = 0.005$ sec seems to provide optimal efficiency.

Post-Buckling Deformation

After the initial limit point at about a 1% shortening of the mast, the simulations exhibit an essentially constant force in the cable over a range of about the next 9% of stowage. This agrees qualitatively with the experiments by Natori *et al.* (1986). Thus interest centers on the evolving global features of the resulting kinematics during this post-buckling stage. These deformation patterns are characterized by the displacements parallel to the mast's axis of the nodes that lie on the axis, i.e., of the centers of the integrated spacers. Figures 2 and 3 show the time histories of these displacements at the one- and two-thirds points of the axis for the models with quadratic and cubic elements, respectively. (The displacements at full height are not shown since they are entirely enforced by the length of the retracting cable.) Results obtained for the axis-aligned rotations exhibit similar patterns and comparisons but are not shown here for brevity.

The post-buckling deformations illustrated in Figures 2 and 3 exhibit some expected and some surprising trends. The computed kinematics depend only weakly on whether quadratic or cubic rod elements are employed; this convergence with respect to spatial discretization is expected because strain-related deformations remain small within individual elements over the time interval studied. Temporal discretization, by contrast, appears far from convergent; indeed, the three smallest time increments produce three clearly distinct post-buckling deformation patterns.

That simulations employing relatively small time increments yield so dissimilar results is hard to reconcile with the frequency content of the simulated kinematics, which has a highest significant contribution of roughly 20Hz. The source of this effect is suggested, however, by a fortuitous numerical accident: for the two extreme time-increment values employed, Δt = 0.001sec and Δt = 0.01sec, the cubic rod model produces essentially the same deformation pattern in the sense that divergence over time between the two simulations is very small and is oscillatory, Figure 3.

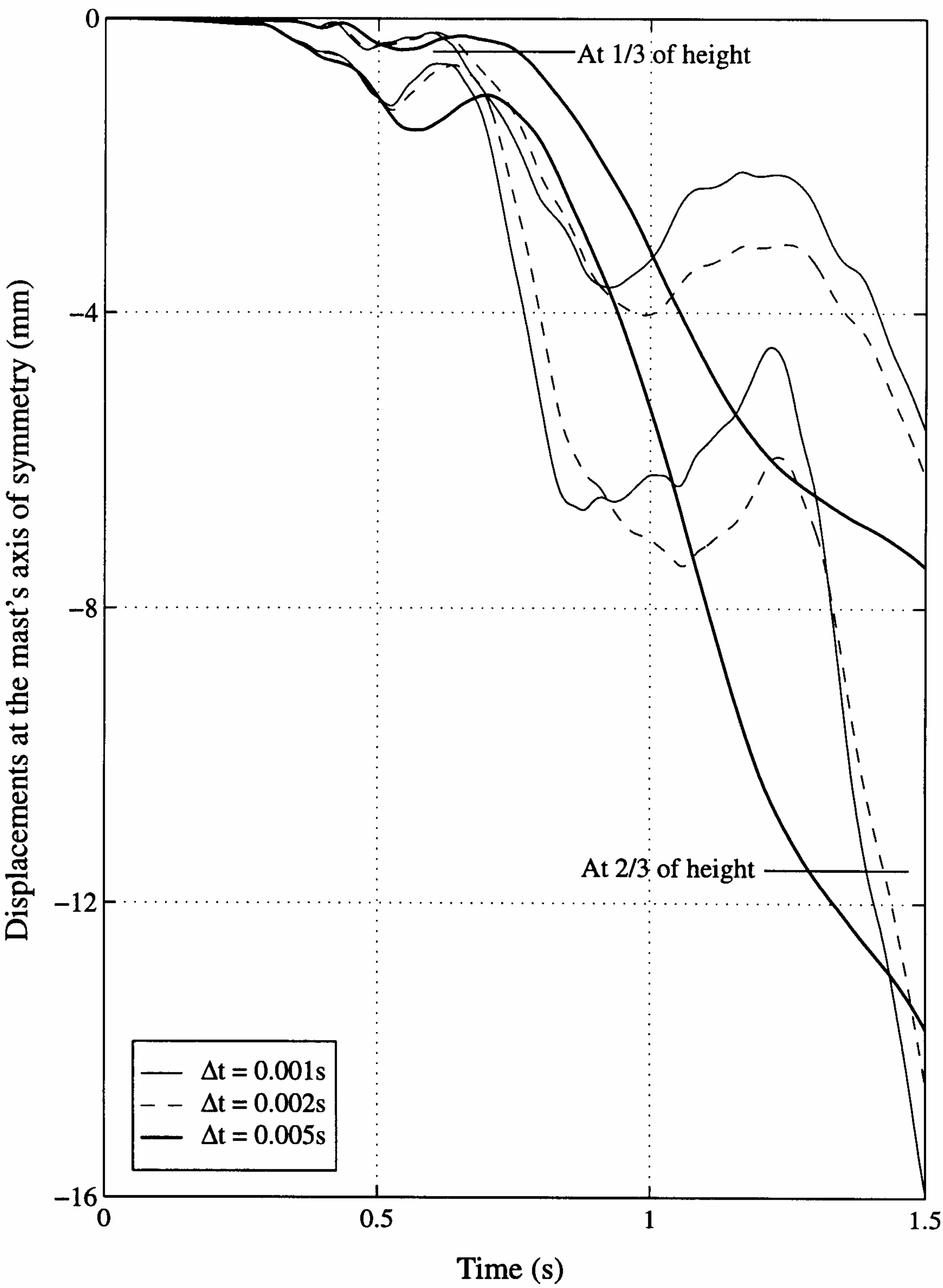

Figure 2. Time history of displacements along mast axis for quadratic-element model

In summary, the simulations depicted in Figures 2 and 3 (and in the omitted comparable figures of post-buckling rotations):

- differ algorithmically only in the time increment employed and in the resulting dissipation of high frequencies by the α-method;

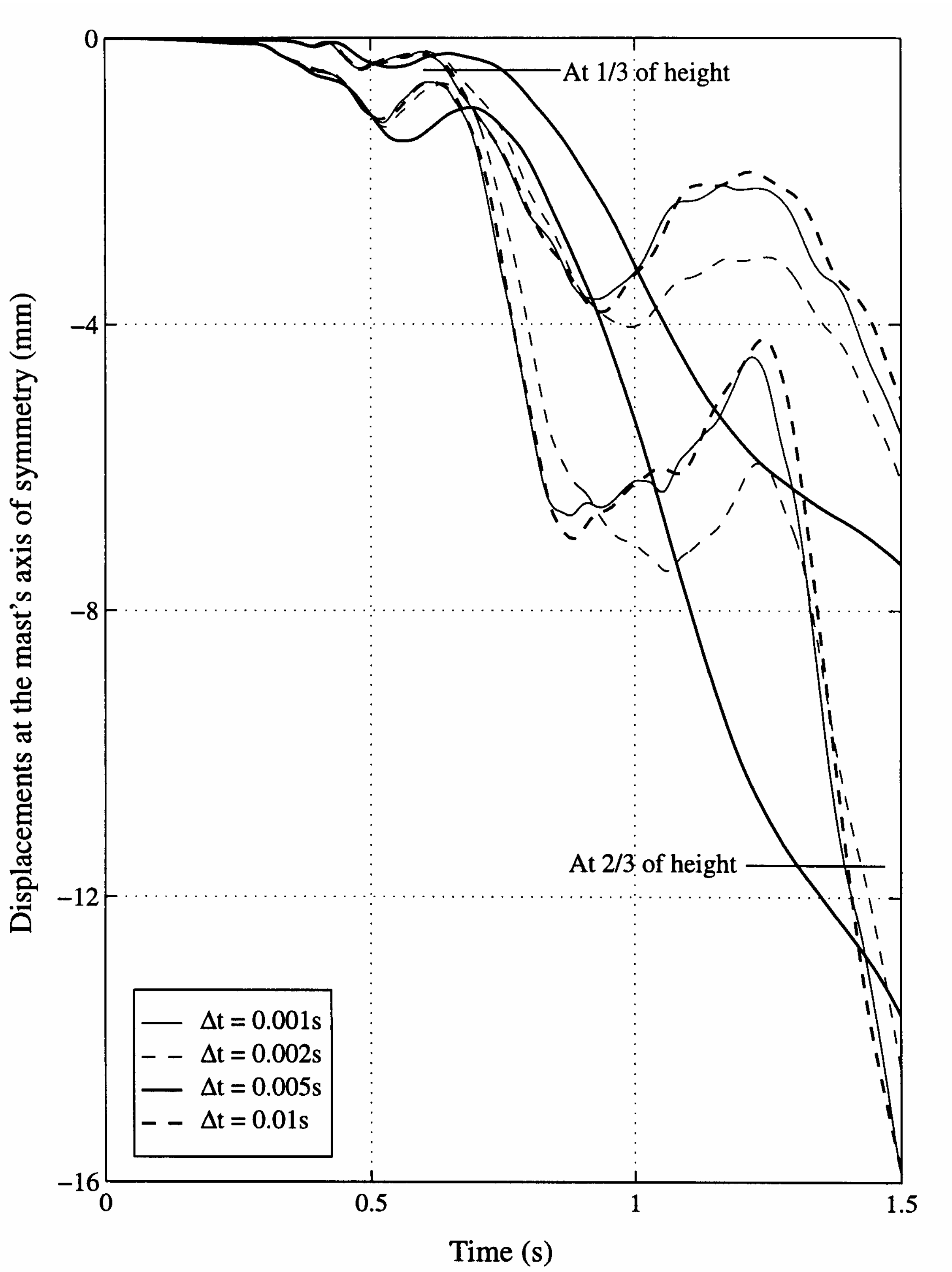

Figure 3. Time history of displacements along mast axis for cubic-element model

- do not accumulate errors by accepting quasi-equilibrium configurations, except in a few isolated cases of low residual;
- enforce the same stowage program which does not significantly excite frequencies beyond 20Hz;

- result in cable-force histories that are essentially identical in magnitude and dynamic behavior; and
- give rise, nevertheless, to three vastly different deformation patterns which originate at the first limit point or shortly thereafter, diverge exponentially, and persist over a significant time interval.

Thus the source of divergent kinematics for different time increments is identified as lack of invertibility in the neighborhood of the limit point.

The sensitivity to initial conditions evident in the numerical results discussed above is in complete agreement with the experimental results reported by Natori *et al.* (1986). These observations indicated that each tested hingeless mast exhibited specific intervals of the statically enforced deployment ratio over which multiple stable equilibria were possible, characterized by almost identical deployment forces and vastly different deformation patterns. It is also reported that one such interval often followed immediately after the first limit point and that, in some occasions, closely spaced static equilibria persisted in parallel over significant deployment intervals.

CONCLUSIONS

The case study selected provides, by virtue of its complexity, a severe test for element formulations, analysis algorithms, and their interaction. By the nature of the problem, the elements used must be geometrically exact, and the low-order, numerically integrated C^0 rod formulations used here have been demonstrated elsewhere (Balopoulos 1997) to model large rigid-body and strain-related deformations accurately. This test case sheds further light on the relative cost and efficiency of the quadratic and cubic order elements.

The variety of nonlinear behavior exhibited by the stowage and deployment of the recoilable mast includes not only progressive softening or stiffening of individual members but discontinuities in tangents, residuals, and even topology (contact). Furthermore, numerical ill-conditioning of the tangent and equilibrium predictors outside of the solution's basin of attraction are probable occurrences. In contending with such conditions, nonlinear system solvers:

- must without exception iterate for equilibrium;
- may not use incremental, tangent-based definitions of the residual;
- must employ step-safeguarding techniques to avoid divergence;
- must monitor and adapt the attempted time increment to ensure convergence, accuracy, and efficiency; and
- must detect discontinuities, determine their time of occurrence, and establish equilibrium immediately before and after them.

Although the solver applied to this case study implements the first three of these, the divergent results for different time increments arises at least in part from the absence of the last two.

Tangent factorizations dominate the computation effort in the simulation of the hingeless mast even though the problem is of modest size and a vector quasi-Newton solver is employed. Possible refinements for improving efficiency include using the same factorized tangent for multiple increments and employing iterative, truncated linear system solvers with infrequently computed approximate tangent factorizations as preconditioning.

The difficulties encountered in simulating the stowage of the hingeless mast serve to highlight limitations of the finite element method as applied to highly nonlinear structural dynamics. These limitations include the restriction that computational resources place on the accuracy of models and their simulations and, more particularly, the sensitivity to initial conditions (bifurcation, closely spaced equilibria, exponential separation). The latter may preclude individual simulations from being representative, as implicitly intended, of the ensemble of responses of a "small neighborhood" of models to a "small neighborhood" of excitations.

It is possible, as is the case for the mast stowage example, for an ensemble of responses to exhibit relatively few and persistent behaviors. In such circumstances, a single simulation of high accuracy is less useful than a set of less accurate ones because the latter have a higher probability of capturing, at least qualitatively, the characteristic behaviors in the ensemble. However, multiple approximate simulations are not always feasible; they may become prohibitively expensive in the presence of severe discontinuities such as widespread and intermittent contact which require drastic reduction in the spatial and temporal discretizations.

ACKNOWLEDGEMENTS

Portions of this work have been sponsored by the U. S. Air Force Office of Scientific Research under Grants No. AFOSR-90-0211 and F49-620-94-1-0129.

REFERENCES

Balopoulos, V. D. (1997), Object-oriented finite-element dynamic simulation of geometrically nonlinear space structures, Ph.D. dissertation, Cornell University.

Golub, G. H., and VanLoan, C. F. (1989), *Matrix Computations*, Johns Hopkins University Press, Baltimore, Maryland.

Hilber, H. M., Hughes, T. J. R., and Taylor, R. L. (1977), Improved numerical dissipation for time integration algorithms in structural dynamics, *Earthquake Engineering and Structural Dynamics* **5**, 283-292.

Hoff, C., Hughes, T. J. R, Hulbert, G., and Pahl, P. J. (1989), Extended comparison of the Hilber-Hughes-Taylor α-method and the Θ_1-method. *Computer Methods in Applied Mechanics and Engineering* **76**(1), 87-93.

Kitamura, T., Okazaki, K., Natori, M., Miura, K., Sato, S., and Obata, A. (1988), Development of a "hingeless mast" and its applications. *Acta Astronautica* **17**(3), 341-346.

Natori, M., Okazaki, K., Sakamaki, M., Tabata, M., and Miura, K. (1986), Model study of simplex masts. *15th International Symposium on Space Technology Science*, Tokyo, 489-496.

Simo, J. C., and Vu-Quoc, L. (1988), On the dynamics of space rods undergoing large overall motions – A geometrically exact approach. *Computer Methods in Applied Mechanics and Engineering*, **66**(2), 125-161.

Simo, J. C., and Vu-Quoc, L. (1991), A geometrically exact rod model incorporating shear and torsion-warping deformation. *International Journal of Solids and Structures*, **27**(3), 371-393.